MILLEDGE, N. J. & PANT, L. M. (1960). *Acta Cryst.* **13**, 285–290.
PAUL, I. C. & CURTIN, D. Y. (1973). *Acc. Chem. Res.* **6**, 217–225.
PAWLEY, G. S. (1967). *Phys. Stat. Sol.* **20**, 347–360.
PAWLEY, G. S. (1972). *Phys. Stat. Sol.* (*b*) **49**, 475–488.
PIERMARINI, G. J. & BRAUN, A. B. (1973). *J. Chem. Phys.* **58**, 1974–1982.
POLTEV, V. I. & SUKHORUKOV, B. I. (1968). *J. Struct. Chem.* **9**, 234–239.
RABINOVICH, D. & SCHMIDT, G. M. J. (1966). *Nature, Lond.* **211**, 1391–1393.
ROBERTSON, J. M., SHEARER, H. M. M., SIM, G. A. & WATSON, D. G. (1962). *Acta Cryst.* **15**, 1–8.
ROSSELL, H. J. & SCOTT, H. G. (1973). *J. Cryst. Mol. Struct.* **3**, 259–270.
RUSH, J. J. (1967). *J. Chem. Phys.* **47**, 3936–3943.
RUSH, J. J. & TAYLOR, T. I. (1966). *J. Chem. Phys.* **44**, 2749–2754.
SASADA, Y. & ATOJI, M. (1953). *J. Chem. Phys.* **21**, 145–152.
SASADA, Y. & ATOJI, M. (1959). *J. Chem. Phys.* **30**, 1103.
SHMUELI, U. & GOLDBERG, I. (1973). *Acta Cryst.* **B29**, 2466–2471.
SIMONETTA, M. (1974). *Acc. Chem. Res.* **7**, 345–350.
STEER, R. J., WATKINS, S. F. & WOODWARD, P. (1970). *J. Chem. Soc. C*, pp. 403–408.
STRELTSOVA, I. N. & STRUCHKOV, Y. T. (1961). *J. Struct. Chem.* **2**, 296–308.
TANAKA, I., IWASAKI, F. & AIHARA, A. (1974). *Acta Cryst.* **B30**, 1546–1549.
THOMAS, J. M. (1974). *Phil. Trans.* **A277**, 251–286.
TULINSKY, A. & WHITE, J. G. (1958). *Acta Cryst.* **11**, 7–14.
VAN STEENWINKEL, R. (1969). *Z. Naturforsch.* **24a**, 1526–1531.
WHEATLEY, P. J. (1957). *Acta Cryst.* **10**, 182–187.
WHEATLEY, P. J. (1960). *Acta Cryst.* **13**, 80–85.
WILLIAMS, D. E. (1966*a*). *Acta Cryst.* **21**, 340–349.
WILLIAMS, D. E. (1966*b*). *J. Chem. Phys.* **45**, 3770–3778.

Acta Cryst. (1975). A**31**, 654

The Topotaxy of the Solid-State Crystal Growth of the Spinel $MgGa_2O_4$ from Its Constituent Oxides*

BY GERALD KATZ
Department of Materials Engineering, Technion – Israel Institute of Technology, Haifa, Israel

AND RUSTUM ROY
Department of Geochemistry and Mineralogy, The Pennsylvania State University, University Park, Pennsylvania 16802, *U.S.A.*

(*Received* 29 *August* 1974; *accepted* 17 *February* 1975)

The topotaxy of the reaction of single crystals of periclase, MgO, and β-Ga_2O_3 to form the spinel $MgGa_2O_4$ was investigated by optical and X-ray diffraction techniques after reaction at 1600°C. Three different reaction couples were studied, namely the (001) face of β-Ga_2O_3 contacting the (001), (110) and (111) surfaces of MgO. The three-dimensional coherency of the oxygen arrangement and packing between each constituent oxide and the spinel reaction product was demonstrated. In both cases the close-packed oxygen planes in the spinel product were aligned parallel to the close-packed oxygen planes in the respective reactant. The topotaxies between the spinel product and the parent crystals were: (*a*) $(111)_{sp}\|(013)_{ga1}$, $[1\bar{1}0]_{sp}\|[100]_{ga1}$; (*b*) $(111)_{sp}\|(111)_p$, $[1\bar{1}0]_{sp}\|[1\bar{1}0]_p$. The data for the topotaxy of the spinel reaction product with respect to β-Ga_2O_3 is fully consistent with an earlier study of the precipitation of β-Ga_2O_3 from a spinel crystalline solution. This study verified a Wagner-type reaction mechanism where the close-packed oxygen anion structure remains essentially unchanged while the reaction proceeds by a counter diffusion of Mg^{2+} and Ga^{3+} ions through the spinel layer formed at the interface. This method of solid-state crystal growth for binary oxide systems at a temperature far below the solidus temperature ($\simeq$2000°C) can find application in the growth of crystals that decompose or melt incongruently or that have an undesirable polymorph when solidified directly from the melt.

1. Introduction

The feasibility of single-crystal growth by solid-state reaction below the solidus temperature has recently been demonstrated by the authors (Katz, 1965; Katz & Roy, 1970). Those results were the outgrowth of an earlier study of topotaxy in the solid-state precipitation of the β-Ga_2O_3 structure from a spinel host crystal, a $MgGa_2O_4$–Ga_2O_3 crystalline solution (Katz, 1965; Katz, Nicol & Roy, 1969*a*,*b*). This was the first instance of the prepicitation of a structure, other than the corundum type, from a spinel crystalline solution. In particular, monoclinic β-Ga_2O_3 (Kohn, Katz & Broder, 1957) was exsolved topotactically from a

---

* This study was performed at the Materials Research Laboratory, The Pennsylvania State University, University Park, Pennsylvania, U.S.A.

spinel matrix. The topotaxy for the precipitation reaction was shown to be:

$$(111)\ \text{spinel} \| (013)_{\beta\text{-gallium oxide}};$$

$$[1\bar{1}0]_{\text{spinel}} \| [100]_{\beta\text{-gallium oxide}}.$$

The $(111)_{\text{spinel}}$ and $(013)_{\beta\text{-gallium oxide}}$ planes are perpendicular to the cubic close-packed directions in the respective structures.

The purpose of this investigation was to see whether the reverse procedure of reacting two oriented single crystals of the constituent oxides MgO and β-Ga_2O_3 would result in a similar topotaxy between the reaction product, the spinel $MgGa_2O_4$, and the reactants. In addition, it would be interesting to learn what effect, if any, the relative orientation of the reacting crystals had on the resultant spinel.

2. Experimental procedures

Single crystals of magnesium oxide were obtained with a purity of 99·9% or better.* Slices of MgO crystals approximately 0·5 mm thick were prepared with the largest surface parallel to (001), (110) and (111). The (001) crystal surfaces were easily obtained from the perfect cubic cleavage of MgO. These surfaces were not polished in any way. The (110) and (111) surfaces were cut with an ultrasonic impact grinder and a boron carbide cutting agent after the crystals had been properly oriented by the Laue back-reflection method. These surfaces were then polished with 600 grit SiC powder. The final orientation of the prepared surfaces was within 0·5° of the desired plane.

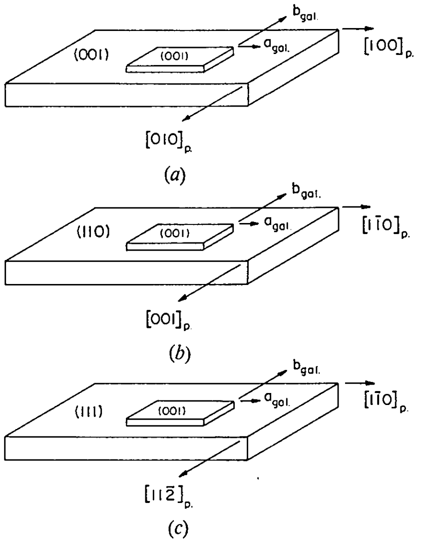

Fig. 1. Crystallographic relationships of reaction couples: (*a*) $(001)_p \| (001)_{gal}$; (*b*) $(110)_p \| (001)_{gal}$ (*c*) $(111)_p \| (001)_{gal}$.

The β-Ga_2O_3 crystals used were those previously described as grown from a lead fluoride flux (Katz & Roy, 1966). Although the β-Ga_2O_3 crystals used were larger than any flux-grown crystals reported in the literature, their small size precluded their orientation and cutting to any desired crystallographic direction. Owing to the perfect (001) cleavage,* crystals tabular on (001) were readily available for the reaction studies. These cleavage surfaces were not polished in any way. All the reaction studies were limited to having (001) as the β-Ga_2O_3 contacting surface.

Three couples were prepared with (001) of β-Ga_2O_3 contacting, respectively, (001), (110) and (111) of MgO. In general the β-Ga_2O_3 crystals were approximately 3 mm in length and the MgO crystals approximately 8 mm in length. Each couple was individually wrapped in platinum foil to maintain contact and suppress any vapor loss of the Ga_2O_3. The orientation relationships of the three couples, as shown in Fig. 1, may be described as follows:†

(*a*) $(001)_p \| (001)_{gal}$
$[100]_p \| [100]_{gal}$

(*b*) $(110)_p \| (001)_{gal}$
$[1\bar{1}0]_p \| [100]_{gal}$

(*c*) $(111)_p \| (001)_{gal}$
$[1\bar{1}0]_p \| [100]_{gal}$.

The couples were introduced into a vertical 100% rhodium-wound furnace operating at 1600°C with a proportional-type controller. The specimen temperature was measured with a 60Rh40Pt *vs.* 20Rh80Pt thermocouple. The temperature was estimated to be correct within ±5°C. Samples were kept at 1600°C for two days and then removed from the furnace and allowed to cool to room temperature.

Evaluation of the reaction products was made with the metallographic and petrographic microscopes and X-ray diffraction methods. Identification of the reaction products and determination of their orientation with respect to the parent or host crystals were made with rotation and Weissenberg X-ray techniques with Ni-filtered Cu *K* radiation.

3. Results and discussion

3.1 *Reaction couple* $(001)_p \| (001)_{gal}$

3.1.1 β-Ga_2O_3 *host crystal*

Inspection of the reaction couple after removal from the furnace indicated that a reaction, presumably forming spinel, had taken place at both contacting faces of the couple. However there was no adherence between the two spinel layers. A fragment of the β-Ga_2O_3 half of the couple photographed under

---

* Semi-Elements, Inc., Saxonburg, Pennsylvania, U.S.A.

* The unit cell edges are labeled according to the convention of Kohn, Katz & Broder (1957): $a = 5{\cdot}80$, $b = 3{\cdot}04$, $c = 12{\cdot}23$ Å, $\beta = 103{\cdot}7°$.

† p = periclase (MgO); gal = β-gallia (β-Ga_2O_3).

crossed Nicols is shown in Fig. 2. The bright birefringent areas exhibited parallel extinction while the darker outlined area was isotropic. This indicated that part of the original β-Ga_2O_3 crystal still remained unreacted while the isotropic regions were the spinel reaction product.

A rotation photograph was taken of the isotropic end of this fragment with the axis of rotation parallel to the long dimension. The unit-cell dimension was determined from the 10,2,2 reflection measured on the equatorial layer line and found to be 8·274 Å which compares favorably with the reported value of 8·280 Å (Swanson, Cook, Evans & De Groot, 1960) for $MgGa_2O_4$. Examination of the zero-layer Weissenberg photograph indicated that the indices of the observed reflections conform to the spinel space group.

A rotation photograph, taken of the crystal (Fig. 2) after the birefringent crystal region was placed in the X-ray beam, is shown in Fig. 3. This was accomplished by translating the crystal along the earlier rotation axis without disturbing the setting on the goniometer head. The main pattern present is one for spinel with $[1\bar{1}0]$ as rotation axis. Inspection of the layer lines indicates that in addition to the intense and somewhat broadened spinel reflections, many sharp well-resolved reflections are observed. These reflections evidently belong to the remaining unreacted β-Ga_2O_3 crystal. The coincidence of the β-Ga_2O_3 and spinel reflections on the same layer lines is due to the very similar periodicities in spinel and β-Ga_2O_3. The spinel periodicity, for a $[1\bar{1}0]$ rotation axis, of 5·85 Å is very close to the a unit-cell edge for β-Ga_2O_3 of 5·80 Å which is the rotation axis for the birefringent phase.

As expected from observations of the rotation photograph, the zero-layer Weissenberg pattern of the two-phase region represents a superposition of the zero layers for β-Ga_2O_3 and spinel. A portion of the reciprocal lattice (R. L.) constructed from the data of the Weissenberg photograph of the birefringent two-phase region (Fig. 2) is given in Fig. 4. The R. L. vectors were calculated using the unit-cell dimensions for β-Ga_2O_3 and the measured unit-cell size for $MgGa_2O_4$.

The diagram represents the superposition of the host β-Ga_2O_3 and the spinel product reciprocal lattices. From the coincident R. L. directions and knowledge of the rotation axes for each phase, the topotaxy of the spinel product as related to the β-Ga_2O_3 host crystal can readily be determined as follows:

$$C_{sp} \| c^*_{gal} = c_{gal} \sin\beta = d_{001gal}$$

$$[1\bar{1}0]_{sp} \| a_{gal}$$

$$[110]_{sp} \| b_{gal}\,.$$

This proved to be identical with the topotaxy previously determined in the case where β-Ga_2O_3 was precipitated from a spinel crystalline solution.

For a transformation to proceed topotactically, there should be a three-dimensional similarity between the structures of the reactants and the product. The size and charge of the ions partly determine which ions move and which do not. In close-packed oxides with small cations, *e.g.* Mg^{2+}, $Al_3{}^+$, Ga^{3+}, Fe^{3+}, Si^{4+}, the oxygen framework tends to stay relatively unchanged while the cations migrate. The number of oxygens per unit volume tends to remain constant in the regions where topotactic transformation takes place.

The topotactic results give the dimensional relationships of the coexistent β-Ga_2O_3 host and spinel product in Table 1.

Table 1. *Dimensional relationships of the* β-Ga_2O_3 *host and spinel product*

Spinel		β-Ga_2O_3
d_{110} (5·85 Å)	$\simeq$	a(5·80 Å)
d_{110} (5·85 Å)	$\simeq$	$2b$(6·08 Å)
$3a$ (24·82 Å)	$\simeq$	$2d_{001} = (2c \sin\beta) = 23{\cdot}78$ Å
$\beta = 90°$		$\beta = 103{\cdot}7°$

It is now possible to determine a transformation volume unit for the host β-Ga_2O_3 crystal and relate it to an equivalent volume in the spinel reaction product. If these equivalent volumes can be shown to contain the same number of oxygen anions then there will be substantial evidence that during the reaction process, the oxygen framework remains fairly fixed and only the smaller cations Mg^{2+}, Al^{3+} and Ga^{3+} migrate. The respective transformation volumes are:

$$V_{sp} = 3a \cdot \frac{a}{\sqrt{2}} \cdot \frac{a}{\sqrt{2}} = 848 \text{ Å}^3$$

$$V_{gal} = 4\; a\,.\,b\,.\,c\,.\,\sin\beta = 842 \text{ Å}^3$$

$$\text{with } \Delta V = +0{\cdot}8\,\%\,.$$

This insignificant volume change may be neglected, especially when one considers the large counter diffusion or rearrangement of cations occurring during

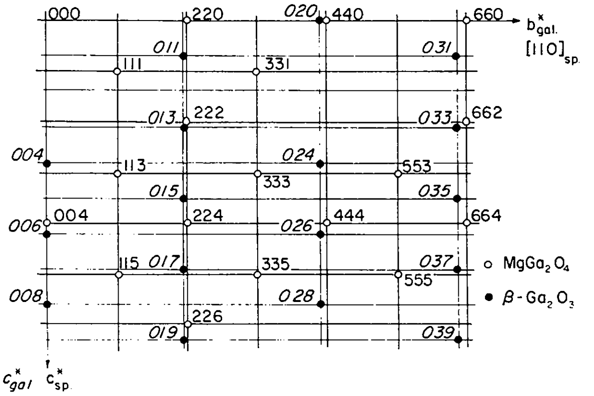

Fig. 4. Portion of zero-layer reciprocal lattice of β-Ga_2O_3 host and spinel reaction product.

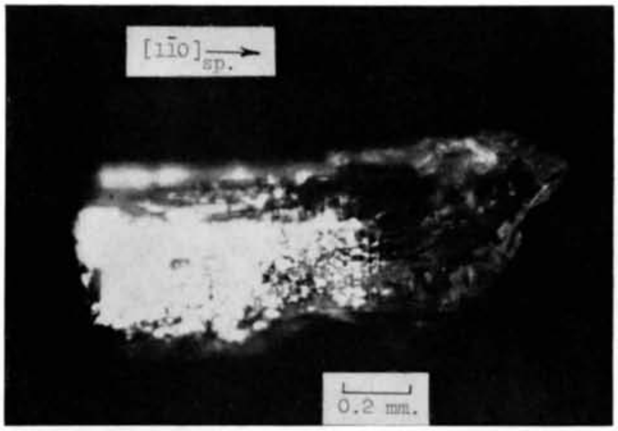

Fig. 2. Fragment of β-Ga_2O_3 host crystal and spinel product. Crossed Nicols, light areas–birefringent, dark areas–isotropic.

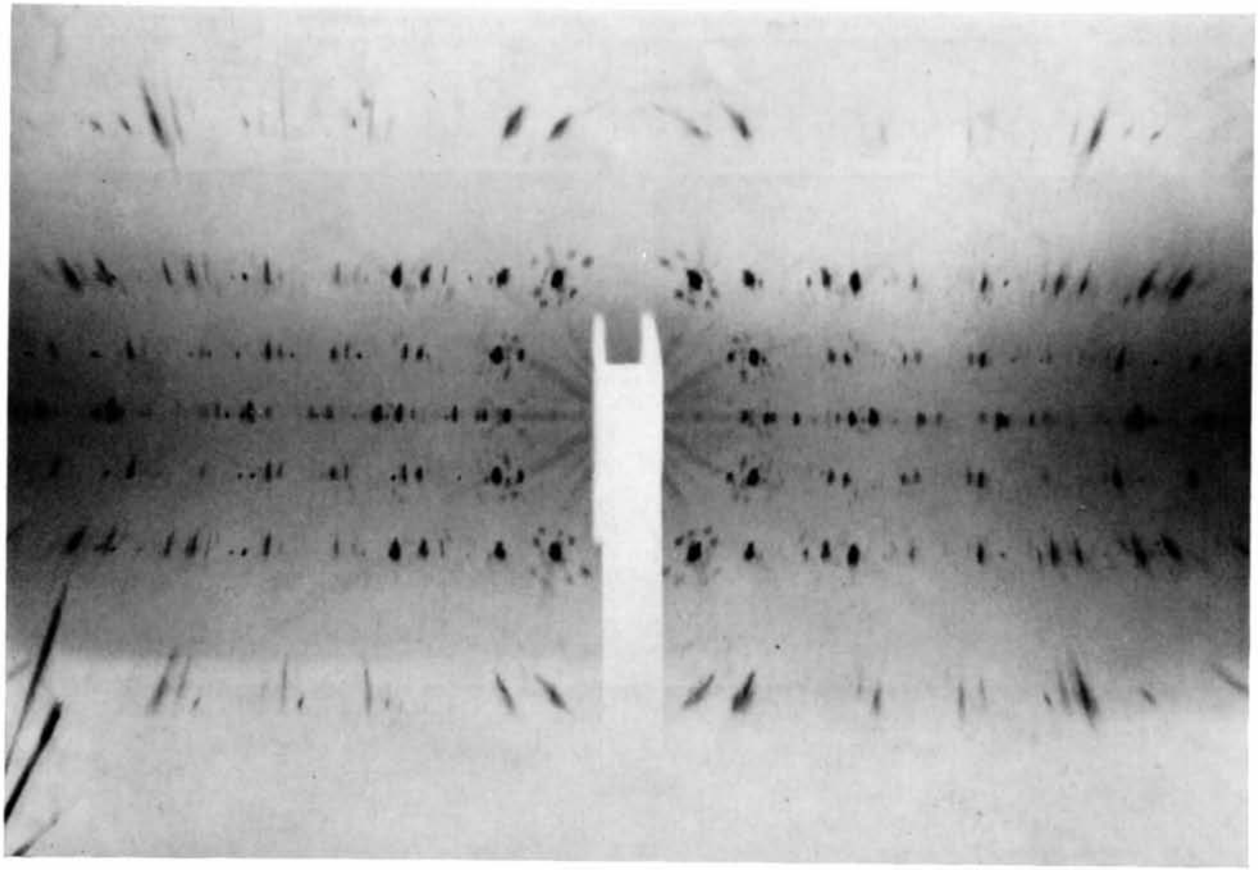

Fig. 3. Rotation photograph of β-Ga_2O_3 host crystal and spinel reaction product, a_{gal} and $[1\bar{1}0]_{sp}$ rotation axes.

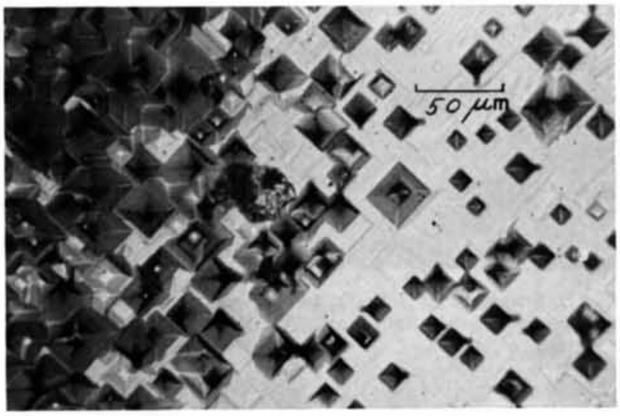

Fig. 6. Spinel octahedra formed on (001) crystal face of MgO host by diffusion (left side) and vapor transport (right side); reflected light.

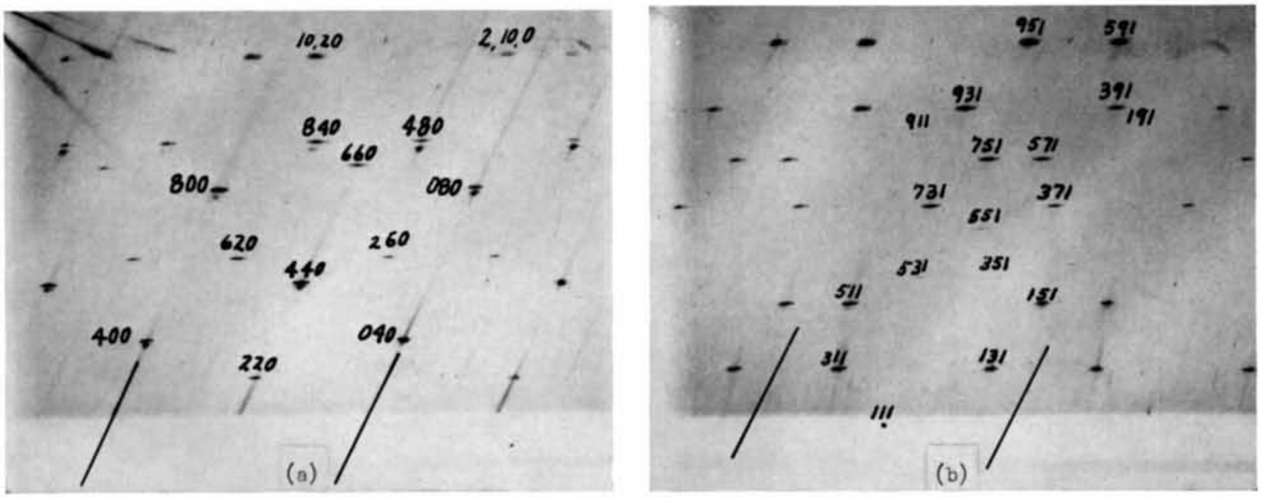

Fig. 7. Weissenberg photographs of the $MgO/MgGa_2O_4$ reaction interface, rotation axis $[001]_p$: (*a*) zero-layer; (*b*) first-layer.

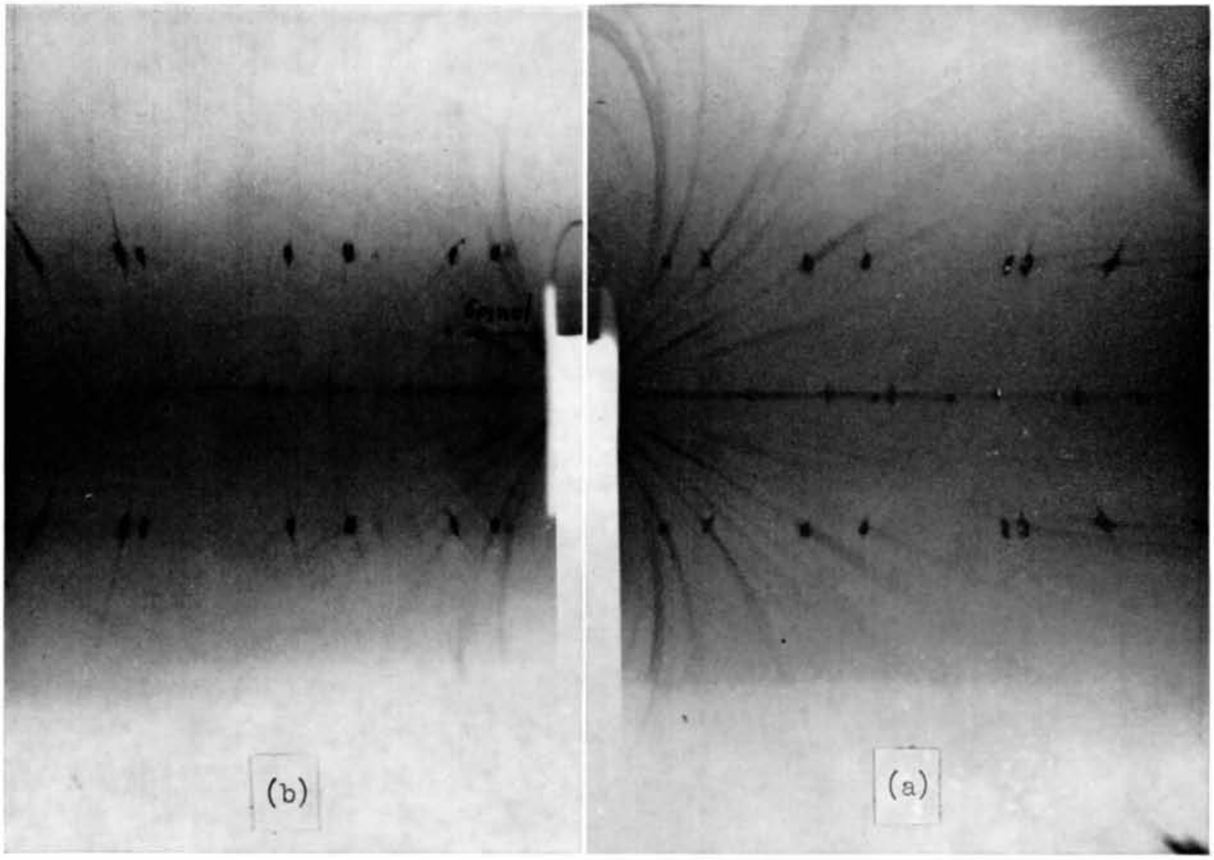

Fig. 8. Rotation photographs of MgO host crystal, [1$\bar{1}$0] rotation axis: *(a)* before reaction–periclase; *(b)* after reaction–periclase + spinel (weak reflections).

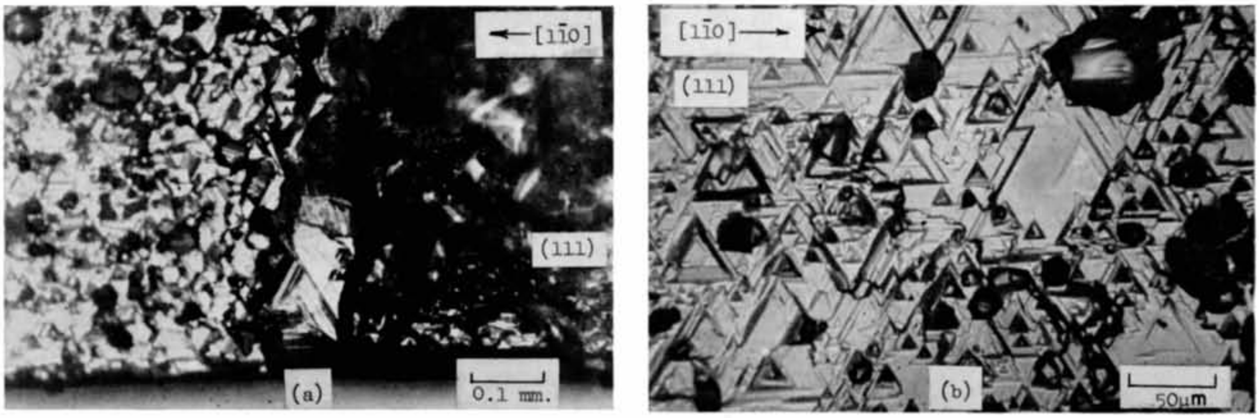

Fig. 9. Spinel reaction product on MgO (111) face, reflected light: *(a)* diffusion and vapor transport region; *(b)* vapor transport region.

the reaction. It now remains to be shown whether the oxygen count for the equivalent transformation volumes remains unchanged. Brindley (1963) has treated at some length the requirement of the constancy of oxygen in equivalent transformation volumes in topotactic reactions. In this instance the oxygen counts in the equivalent transformation volumes are identical:

$$\beta\text{-Ga}_2\text{O}_3\ 4\,.\,4\,.\,\text{O}_3=48\ \text{O}^{2-}$$

$$\text{Spinel}\ 1{\cdot}5\,.\,8\,.\,\text{O}^4=48\ \text{O}^{2-}\,.$$

The essentially equal transformation volumes with identical oxygen counts verify the transformation as a topotactic one with only slight rearrangement, if any, of the close-packed oxygen framework taking place.

The oxygen arrangements in β-Ga$_2$O$_3$ and MgGa$_2$O$_4$ spinel are shown in Fig. 5(*a*), in the previously determined relative orientation, as projected on a common plane. The atomic parameters of Geller (1960) served to determine oxygen positions for β-Ga$_2$O$_3$. For spinel, the ideal parameter $u=0{\cdot}375$ was used for determining the oxygen positions. The separation of the oxygen layers in spinel along [110] is

$$\frac{a_{\text{sp}}\sqrt{2}}{8}=1{\cdot}46\ \text{Å}\,.$$

This value is in good agreement with the distance ($b/2$) between the oxygen layers along the $[010]_{\text{gal}}$ direction of 1·52 Å. The separation of the oxygen layers in spinel along the a axis is

$$a_{\text{sp}}/4=2{\cdot}07\ \text{Å}$$

as compared to a mean spacing of the equivalent oxygen planes in β-Ga$_2$O$_3$ of

$$d_{001}/6=1{\cdot}99\ \text{Å}\,.$$

Fig. 5(*b*) represents an end view as seen down the a_{gal} and $[1\bar{1}0]_{\text{sp}}$ directions. Again, the similarity of the oxygen arrangements in both structures is very apparent.

The foregoing analysis of the similarity of the three-dimensional oxygen arrangement in both the host or parent crystal and the reaction-product crystal is in very good agreement with the theories of coherent precipitation advanced some time ago by Cottrell (1955) and Barrett (1952). They dealt primarily with the solid-state precipitation and crystal growth of a second phase in a host crystal upon cooling and discussed the reduction of the interfacial free energy component of the precipitation reaction. It is believed that their treatment is applicable to the case in question, of a reaction mechanism forming a new phase from two reactants, albeit that the systems considered by these authors were less complex than the case under study. Theirs was the relatively simpler case for metals and alloys where primitive translation vectors defining the unit cell can be chosen so that one deals with only a single atom per unit cell. For this reason only the oxygen arrangement, for which there are some 32 and 12 atoms per unit cell of spinel and β-Ga$_2$O$_3$ respectively, has been considered in the present case while the cations have been neglected. Since these are essentially close-packed oxygen structures, it is the coherence of the oxygen planes that has been considered. It now seems evident from the present study that the coherent type of low-energy interface, relatively dislocation free, presents itself in this reaction mechanism.

Although it is not a necessary prerequisite for a topotactic precipitation or transformation, very often the close-packed oxygen planes of the precipitate and host crystal are aligned parallel to each other (Brindley, 1963). This is true where the corundum structure precipitates from the spinel structure (Saalfeld & Jagodzinski, 1957; Carter, Roth & Julien, 1959; Saalfeld, 1962). In the decomposition of brucite [Mg(OH)$_2$], similarly, the final MgO product has its close-packed oxygen planes parallel to those in the starting crystal (Büssem & Köberich, 1932). The same phenomenon was observed for the maghemite (γ-Fe$_2$O$_3$) to hematite (α-Fe$_2$O$_3$)

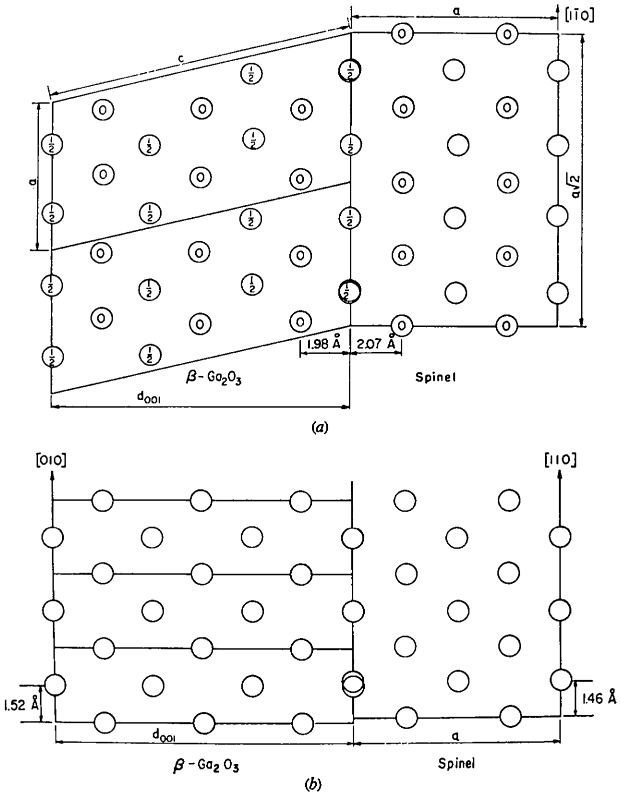

Fig. 5. Similarity of oxygen arrangement in β-Ga$_2$O$_3$ and spinel. (*a*) oxygen arrangement as projected on (010) of β-Ga$_2$O$_3$ and (110) of spinel. Oxygen anions in β-Ga$_2$O$_3$ marked O are located on (010), others are positioned at $b/2$ (1·52 Å) above (010). Oxygen ions in spinel marked O represent layer at same reference height as those similarly marked for β-Ga$_2$O$_3$. Unmarked oxygen ions in spinel represent next-highest layer above the O layer. (*b*) End view of (*a*) as seen down a_{gal} and $[1\bar{1}0]_{\text{sp}}$.

transformation by Bernal, Dasgupta & Mackay (1959). In the case where monoclinic β-Ga_2O_3 is the precipitating phase, its close-packed oxygen planes (013), as well, lie parallel to the (111) oxygen planes in spinel. The interplanar spacing of the close-packed oxygen layers parallel to (013) of β-Ga_2O_3 was calculated as $d_{013}=2{\cdot}41$ Å. Assuming ideal cubic close packing, the corresponding separation of close-packed oxygen layers in the [111] spinel direction is 2·39 Å.

The close agreement between the separation of close-packed oxygen layers in the two structures further verifies the topotactic nature of the reaction and the coherency of the spinel formation on the β-Ga_2O_3 parent crystal. The reaction $MgO+\beta\text{-}Ga_2O_3=MgGa_2O_4$ is a topotactic one where there is little rearrangement of the oxygen network, and the reaction is accomplished by the Wagner (1936) mechanism of a counter diffusion of cations through the oxygen framework. The topotaxy of the spinel reaction product on the β-Ga_2O_3 host is identical with the previous results from the precipitation study, *i.e.*

$$(111)_{sp}\|(013)_{gal}$$
$$[1\bar{1}0]_{sp}\|[100]_{gal}\,.$$

3.1.2 MgO *host crystal*

The field of Fig. 6 represents a view normal to (001) face of the MgO parent crystal. The clearly distinguishable octahedra represent spinel formation from the contacting MgO and β-Ga_2O_3 crystals as shown schematically in Fig. 1(*a*). The absence of a birefringent phase indicated that all the β-Ga_2O_3 had been consumed and that there was no residual unreacted β-Ga_2O_3 present. The dense region of octahedra represents the spinel produced by diffusion at the couple interface while the sparsely populated region represents spinel formed after the vapor transport of gaseous Ga_2O_3 products and subsequent diffusion into the periclase crystal at points of sublimation. The octahedra lie above the (001) surface of the MgO crystal and are not depressions due to thermal etching. The orientation of the octahedra is compatible with that of the MgO host crystal, *i.e.*, the apices are aligned with [100] of the MgO substrate.

Since both spinel and periclase are essentially cubic close-packed oxygen structures, observation of the orientation of the spinel octahedra should define the topotaxy with respect to the MgO orientation. Since the edges of the field of Fig. 6 represent {100} faces and since the apices of the octahedra point to these faces, the topotaxy may be defined as:

$$(100)_{sp}\|(100)_p$$
$$[010]_{sp}\|[010]_p\,.$$

The topotaxy for the spinel product and the periclase host was also determined by X-ray Weissenberg goniometry. The sample used in this study was a fragment of the MgO host crystal containing a contiguous spinel reaction product. An axis along the reaction interface, *i.e.* $[100]_p$ [Fig. 1(*a*)], was used as the crystal rotation axis. The zero- and first-layer Weissenberg photographs are shown in Fig. 7. All the labeled indices refer to the $MgGa_2O_4$ unit cell. In the zero-layer photograph, two sets of reflections may be distinguished. One set is horizontally streaked while the other is somewhat circular in character. In addition, all the streaked reflections have a larger 2θ than the circular ones. The two sets of reflections are readily explained if the spinel product and the periclase host have identical orientations. The slight separation between sets of reflections is due to the fact that the $MgGa_2O_4$ unit cell size of 8.280 Å (Swanson, Cook, Evans & De Groot, 1960) is not quite double that of MgO which is 4·213 Å (Swanson & Tatge, 1953). Since spinel and periclase belong to the face-centered space groups *Fd3m* and *Fm3m* respectively, all permissible reflections must meet the requirement that the indices be all odd or all even. Accordingly a check of Fig. 7(*a*) indicates that only for the case where $h/2\ k/2\ l/2$ results in such an index are there two sets of reflections.

Since the unit-cell edge of spinel is approximately double that of periclase, the first layer-line of spinel should not coincide with that for periclase. Indeed this is the case as seen in Fig. 7(*b*) where all reflections have the characteristic streak shape of the spinel phase. None of the indexed reflections can be converted to periclase indices by halving the integers.

The dimensional relationship between $MgGa_2O_4$ and MgO is simply:

$$2a_p(8{\cdot}43\ \text{Å})\simeq a_{sp}(8{\cdot}28\ \text{Å})\,.$$

The comparative unit transformation volumes are $V_p=598$ Å^3 and $V_{sp}=568$ Å^3 with $\Delta V=-5{\cdot}0\,\%$.

The spacings between the close-packed planes, assuming ideal close-packing in both structures, are very similar:

$$\frac{a_p\sqrt{3}}{3}=2{\cdot}43\ \text{Å}$$
$$\frac{a_{sp}\sqrt{3}}{6}=2{\cdot}39\ \text{Å}\,.$$

3.2 *Reaction couple* $(110)_p\|(001)_{gal}$

Examination of this reaction couple after removal from the furnace indicated only a single reaction product on top of the periclase crystal. There were no separate spinel products formed on each of the host crystals. There was no sign of a birefringent phase, indicating that all the β-Ga_2O_3 had reacted to form spinel.

Rotation photographs taken before and after reaction are compared in Fig. 8. The original $[1\bar{1}0]$ periclase direction is the rotation axis. After the reaction, weak but definite spinel reflections appear both on the zero- and first-layer lines. Owing to the almost double periodicity of spinel compared to periclase, a second set of layer lines has appeared. Note the new layer-line approximately midway between the zero- and first-layers of periclase and another layer-line beyond the first layer-line of periclase. Obviously both the spinel reaction product and the periclase host crystal have the same orientation. The topotaxy of this reaction is readily seen to be:

$$(110)_{sp}\|(110)_p$$
$$[1\bar{1}0]_{sp}\|[1\bar{1}0]_p\,.$$

3.3 *Reaction couple* $(111)_p\|(001)_{gal}$

3.3.1 *β-Ga_2O_3 host crystal*

As in the $(001)_p$ reaction couple, after removal from the furnace, two crystal conglomerates were found. One consisted of the periclase host upon which a reaction product could be discerned. The other consisted of a plate-like rectangular fragment, presumably from the β-Ga_2O_3 host. The absence of any birefringent character indicated that the β-Ga_2O_3 host had completely reacted to form $MgGa_2O_4$. The topotaxy was determined from a zero-layer Weissenberg photograph together with the original crystallographic orientation of the reaction couple as shown in Fig. 1(*c*). The X-ray photograph, as well as the resulting topotaxy, were identical to those found for the isotropic spinel crystal described in the $(001)_p$ couple. The $[1\bar{1}0]$ spinel rotation axis was coincident with the original *a* axis of β-Ga_2O_3, giving a topotaxy:

$$(111)_{sp}\|(013)_{gal}$$
$$[1\bar{1}0]_{sp}\|[100]_{gal}\,.$$

3.3.2 MgO *host crystal*

In Fig. 9(*a*) a portion of the periclase crystal is shown normal to the (111) face. The dense black area represents the spinel reaction product which formed by diffusion at the periclase–β-Ga_2O_3 interface. In the lighter region the {111} octahedral faces of spinel formed by vapor-transport reaction can be seen. Since the vapor reaction product forms only a thin layer above the periclase surface, it is out of focus in the photograph. In Fig. 9(*b*) the vapor reaction product is the primary phase shown. The {110} traces of the octahedra are seen to lie in the $[1\bar{1}0]$ direction of both spinel and periclase. The topotactic description of the spinel and periclase host is:

$$(111)_{sp}\|(111)_p$$
$$[1\bar{1}0]_{sp}\|[1\bar{1}0]_p\,.$$

4. Summary and conclusions

A detailed study and analysis of the topotaxy of the formation of $MgGa_2O_4$ from its constituent oxides, MgO and β-Ga_2O_3, has shown that the resulting crystallographic relationships between the reacting crystals and the reaction product were independent of the relative orientation of the reactants. The (001) contacting surface of the β-Ga_2O_3 component, however, was fixed while the contacting surfaces of the MgO component were successively (001), (110) and (111). For all three reaction couples, the topotaxies of the spinel product relative to the respective reactants were found to be:

$$(a)\ (111)_{sp}\|(013)_{gal} \qquad (b)\ (111)_{sp}\|(111)_p$$
$$[1\bar{1}0]_{sp}\|[100]_{gal} \qquad [1\bar{1}0]_{sp}\|[1\bar{1}0]_p\,.$$

In the case of each topotaxy examined, *i.e.* the spinel product as related to each of the two reactants, equivalent transformation volumes have been described where the total oxygen count in each volume is constant. Furthermore, a striking similarity between the three-dimensional oxygen arrangement and packing in both the reactants and reaction product has been demonstrated. In both cases the close-packed oxygen layers of the reaction product are aligned parallel to those in the parent crystals. Table 2 summarizes the unit-cell dimensions and the separation of oxygen layers for the reactants and product relative to the topotaxies found.

Table 2. *Comparison of unit-cell dimensions and oxygen layer separations in* β-Ga_2O_3, MgO *and* $MgGa_2O_4$

β-Ga_2O_3		$MgGa_2O_4$		MgO	
Unit cell	Å	Unit cell	Å	Unit cell	Å
a	5·80	$d_{1\bar{1}0}$	5·85	$2d_{1\bar{1}0}$	5·96
2*b*	6·08	d_{110}	5·85	$2d_{110}$	5·96
$2d_{001}$	23·78	3*a*	24·82	6*a*	25·28
Layer separation		Layer separation		Layer separation	
⊥(013)	2·41	[111]	2·39	[111]	2·43
⊥(010)	1·52	[110]	1·46	[110]	1·49
⊥(001)	1·99	[100]	2·07	[100]	2·11

It is believed that the concepts of coherency as applied to precipitation of metals from solid solutions and subsequently applied to the precipitation of metal oxides from solid or crystalline solutions can also be applied to this study. Once the three-dimensional similarities of the oxygen arrangement in the reactants and the reaction product have been shown for these essentially close-packed oxygen structures, the classical Wagner (1936) mechanism for spinel formation can be applied. Most solid-state reactions can be described as diffusion controlled, whereby the reaction takes place by a counter diffusion of cations of the reactants through the anion network of the product. The reaction in question proceeds only by diffusion of the cations Mg^{2+} and Ga^{3+} in opposite directions through the spinel layer formed at the interface. In the reacting oxides, the larger O^{2-} anions are close-packed while the much smaller cations can diffuse into the oxygen network filling octahedral and tetrahedral interstices to form spinel on each side of the reaction interface.

The three phases involved in the spinel-forming reaction, *i.e.* MgO, β-Ga_2O_3 and $MgGa_2O_4$, are essentially cubic close-packed oxygen structures. This precludes the need for the formation of an intermediate metastable phase whose oxygen arrangement or packing would enable a gradual transition from one type of oxygen packing to another, *e.g.* cubic close-packed to hexagonal close-packed.

It is of interest to note that although there is considerable analogy between topotaxy in metal and oxide systems, no comparable studies have been reported for metal systems for reactions of the type: $A+B \rightarrow C$.

The authors wish to thank Professor G. W. Brindley for his valuable discussions during the course of this investigation and for his critical review of the manuscript. This study was supported by the U.S. Air Force Office of Scientific Research, Solid State Science Division under Grant No. AF-AFOSR-208-63.

References

BARRETT, C. S. (1952). *Structure of Metals*. New York: McGraw-Hill.

BERNAL, J. D., DASGUPTA, D. R. & MACKAY, A. L. (1959). *Clay Mineral Bull.* **4**, 15–30.

BRINDLEY, G. W. (1963). *Prog. Ceram. Sci.* **3**, 1–55.

BÜSSEM, W. & KÖBERICH, F. (1932). *Z. phys. Chem.* **B17**, 310–326.

CARTER, R. E., ROTH, W. L. & JULIEN, C. A. (1959). *J. Amer. Ceram. Soc.* **42**, 533–536.

COTTRELL, A. H. (1955). *Theoretical Structural Metallurgy*, 2nd ed. London: Edward Arnold.

GELLER, S. (1960). *J. Chem. Phys.* **33**, 676–684.

KATZ, G. (1965). *Topotactic Reactions in Precipitation from, and Formation of Gallium Spinels*. Thesis, The Pennsylvania State Univ.

KATZ, G., NICOL, A. W. & ROY, R. (1969*a*). *Nature, Lond.* **223**, 609–610.

KATZ, G., NICOL, A. W. & ROY, R. (1969*b*). *Z. Kristallogr.* **130**, 388–404.

KATZ, G. & ROY, R. (1966). *J. Amer. Ceram. Soc.* **49**, 168–169.

KATZ, G. & ROY, R. (1970). *J. Cryst. Growth*, **6**, 221–227.

KOHN, J. A., KATZ, G. & BRODER, J. (1957). *Amer. Min.* **42**, 398–407.

SAALFELD, H. (1962). *Ber. Dtsch. Keram. Ges.* **39**, 52–54.

SAALFELD, H. & JAGODZINSKI, H. (1957). *Z. Kristallogr.* **109**, 87–109.

SWANSON, H. E., COOK, M. I., EVANS, E. H. & DE GROOT, H. H. (1960). *Standard X-Ray Diffraction Powder Patterns*, Circular 539, **10**, National Bureau of Standards, Washington, D.C.

SWANSON, H. E. & TATGE, E. (1953). *Standard X-Ray Diffraction Powder Patterns*, Circular 539, **1**, National Bureau of Standards, Washington, D.C.

WAGNER, C. (1936). *Z. phys. Chem.* **B34**, 300–316.

Acta Cryst. (1975). A**31**, 660

Transition of V_6O_{13} to VO_2 Observed with a High-Resolution Electron Microscope

BY SHIGEO HORIUCHI, MASANOBU SAEKI AND YOSHIO MATSUI

National Institute for Researches in Inorganic Materials, Sakura-mura, Niihari-gun, Ibaraki, 300·31 *Japan*

AND FUMIO NAGATA

Hitachi Central Research Laboratory, Kokubunji, Tokyo, 185 *Japan*

(*Received* 12 *August* 1974; *accepted* 20 *March* 1975)

Under irradiation by an intense electron beam a V_6O_{13} crystal reacts with the carbon deposited on the surface during microscopic observation. The structural changes during the reaction were directly observed by means of lattice images, in which the array of VO_6 octahedra was resolved. At the initial stage cavities smaller than 20 Å in diameter appear preferentially in the thin part of the crystal and some crystallographic shear planes are formed in their wall. The cavities with the heavily distorted surroundings are seen as white regions. Kinks in lattice fringes, indicating the occurrence of stacking faults, are simultaneously found in the matrix. At the advanced stage the VO_2 phase and its twin component are produced. The mechanism of the transition of V_6O_{13} to VO_2 can be interpreted in terms of the cooperative movement of octahedra.

Introduction

It is known for a vanadium–oxygen system that there are two series of Magnéli phase, *i.e.* V_nO_{2n-1} ($n=3$ to 8) between V_2O_3 and VO_2, and V_nO_{2n+1} ($n=3$ and 6) between VO_2 and V_2O_5 (Andersson, 1954; Stringer, 1965). Tilley & Hyde (1970) reported that a V_2O_5 crystal heated by the irradiation of an intense electron